Applied Surface Science 257 (2011) 3399–3403

Contents lists available at ScienceDirect

Applied Surface Science

journal homepage: www.elsevier.com/locate/apsusc

Surface charging at the (1 0 0) surface of Cu doped and undoped $Li_2B_4O_7$

Jie Xiao[a], N. Lozova[b], Ya.B. Losovyj[a,b], D. Wooten[c], I. Ketsman[a], M.W. Swinney[c], J. Petrosky[c], J. McClory[c], Ya.V. Burak[d], V.T. Adamiv[d], A.T. Brant[e], P.A. Dowben[a,*]

[a] Department of Physics and Astronomy and the Nebraska Center for Materials and Nanoscience, University of Nebraska-Lincoln, Theodore Jorgensen Hall 855 North 16th Street, Lincoln, NE 68588-0299, USA
[b] J. Bennett Johnston Sr. Center for Advanced Microstructures and Devices, Louisiana State University, 6980 Jefferson Highway, Baton Rouge, LA 70806, USA
[c] Air Force Institute of Technology, 2950 Hobson Way, Wright Patterson Air Force Base, OH 45433-7765, USA
[d] Institute of Physical Optics, 23 Dragomanov Str., Lviv 79005, Ukraine
[e] Department of Engineering Physics, West Virginia University, Morgantown, WV 26506, USA

ARTICLE INFO

Article history:
Received 19 March 2010
Received in revised form 3 November 2010
Accepted 4 November 2010
Available online 16 November 2010

PACS:
79.60.Ai
68.55.Ln
29.40.Wk
81.05.J

Keywords:
Oxide dielectric layers
Lithium borate
Surface photovoltaic charging

ABSTRACT

We have compared the photovoltaic charging of the (1 0 0) surface termination for Cu doped and undoped $Li_2B_4O_7$. While the surface charging at the (1 0 0) surface of $Li_2B_4O_7$ is significantly greater than observed at (1 1 0) surface, the Cu doping plays a role in reducing the surface photovoltage effects. With Cu doping of $Li_2B_4O_7$, the surface photovoltaic charging is much diminished at the (1 0 0) surface. The density of states observed with combined photoemission and inverse photoemission remains similar to that observed for the undoped material, except in the vicinity of the conduction band edge.

1. Introduction

With the fabrication of a semiconducting boron carbide, a material suitable for the fabrication of solid state neutron detectors [1–7], there has been a resurgence in the development of boron based semiconductors for neutron detection. In addition to the boron carbides [1–7], possible boron based semiconductors for solid state neutron detectors include boron nitrides [8,9], boron phosphides [10–11], and the lithium borates [12,13]. Although $Li_2B_4O_7$ lithium borate has a much larger (6.3–10.1 eV) band gap [14–20] than the boron carbides, boron nitrides, or boron phosphides, this class of materials has distinct advantages. Because of the large band gap, lithium borates are typically transparent in the range of 165–6000 nm and furthermore can be isotopically enriched to a high degree. $Li_2B_4O_7$ can be isotopically enriched to 95 at% ^{6}Li and 97.3 at% ^{10}B [13] from the natural 7.4 at% ^{6}Li and 19 at% ^{10}B.

Since lithium tetraborate ($Li_2B_4O_7$) single crystals are pyroelectric and piezoelectric [19–22], surface termination and interface effects must be seriously considered in solid state device design. This is a critical consideration as doping will serve to enhance differences along different crystal directions [23]. Doping of the $Li_2B_4O_7$ is certainly possible [13], and essential for solid state neutron detection applications, given the very high resistivities of undoped crystals. The undoped $Li_2B_4O_7$ resistivities are on the order of 10^{10} Ω cm [12], so that doping is essential to both suppress pyroelectricity and increase transport, ideally electron transport as the hole mass is quite large as indicated by the band structure [18,20]. In fact, Cu doping is indeed seen to increase carrier lifetimes [20,24], further indicating the importance of doping for device applications [20].

2. Experimental

The $Li_2B_4O_7$ and $Li_2B_4O_7$:Cu single crystals, both with the natural isotope distribution (^{6}Li – 7.4%, ^{7}Li – 92.6%, ^{10}B – 19% and ^{11}B – 81%), were grown from the melt by the Czochralski technique as described elsewhere [13,15,16]. The Cu dopant centers are seen to be univalent Cu^+ ions in the $Li_2B_4O_7$ lattice, inde-

---

[*] Corresponding author. Tel.: +1 402 472 9838; fax: +1 402 472 2879.
E-mail address: pdowben@unl.edu (P.A. Dowben).

0169-4332/$ – see front matter © 2010 Elsevier B.V. All rights reserved.
doi:10.1016/j.apsusc.2010.11.033

pendent of the valence of Cu in the initial chemical agent used for doping. We doped $Li_2B_4O_7$ single crystals using CuO in the growth mixture, as was done previously [17,25]. The distribution coefficient depends on Cu concentration in the melt, but does not exceed 0.04, and the single crystal $Li_2B_4O_7$:Cu doped samples are nominally $Li_{1.998}Cu_{0.002}B_4O_7$, as determined by quantitative spectrographic analysis. Clean surfaces were prepared by several methods including resistive heating and combinations of sputtering and subsequent annealing. The electronic structure and stoichiometry were similar in all cases [18,19].

Combined ultraviolet photoemission (UPS) and inverse photoemission (IPES) spectra were used to characterize the placement of both occupied and unoccupied states in $Li_2B_4O_7$ single crystals at the (1 0 0) and (1 1 0) surfaces. The temperature-dependent angle-resolved photoemission experiments were performed using the 3 m toroidal grating monochromator (3 m TGM) beam line [26] in an ultra high vacuum (UHV) chamber previously described [18–19,26–28]. Photoemission was conducted over a range of temperatures from 250 to 700 K. Throughout this work, the light incidence angle was 45° but changes were made to the direction of the in-plane component orientation of the $\underline{\mathbf{E}}$ of the plane-polarized incident light. The photoelectrons were collected along the surface normal throughout this work to preserve the high point group symmetry ($\overline{\Gamma}$).

The inverse photoemission (IPES) spectra were obtained by using variable energy electrons incident along the sample surface normal, again to preserve the high point group symmetry ($\overline{\Gamma}$), while measuring the emitted photons at a fixed energy (9.7 eV) using a Geiger-Müller detector with an instrumental linewidth of about 400 meV [18,19,29–30]. The inverse photoemission spectra were taken for sample temperatures of 300–400 K, but no surface charging was observed in the inverse photoemission. Checks to the placement of the Fermi level in both the angle-resolved photoemission and inverse photoemission experiments were performed using tantalum films in electrical contact with the samples. Surface charging shifts in the photoemission were also taken into account by using the Li 1s and O 2s shallow core levels as reference energy levels [19,31].

A Bruker EMX spectrometer operating near 9.48 GHz was used to take EPR data. A helium-gas-flow system maintained the sample temperature near 20 K, and a proton NMR gaussmeter provided values of the static magnetic field. A small Cr-doped MgO crystal was used to correct for the difference in magnetic field between the sample and the probe tips of the gaussmeter (the isotropic g value for Cr^{3+} in MgO is 1.9800). An X-ray tube (operating at 60 kV and 30 mA) was used to convert defects in the $Li_2B_4O_7$ crystals to their paramagnetic charge states. Irradiation times were 30 min.

3. The $Li_2B_4O_7$(1 0 0) valence and conduction band density of states

From Fig. 1, it is clear that for the nominally undoped $Li_2B_4O_7$(1 0 0), the band gaps obtained from combined photoemission and inverse photoemission are 10.1 ± 0.5 eV and 8.9 ± 0.5 eV at the high symmetry $\overline{\Gamma}$ point of each surface, with the in plane component of $\underline{\mathbf{E}}$ aligned along the [0 1 1] and [0 1 0] directions, respectively. This tends to be towards the higher end of the theoretically predicted band gaps that range from 6.2 to 9.7 eV [14–16]. This value determined from the combined photoemission and inverse photoemission is also somewhat larger than the value of 7.4–7.5 eV estimated from the optical absorption edge [17], as expected for photo-excitations due to Coulomb interactions with the photohole. This band gap value, determined from the combined photoemission and inverse photoemission, is in surprisingly good agreement with LDA calculations [14], given that local density approximation (LDA) models will typically underestimate the band gap [32–37]. The experimental estimate of the band gap could also be flawed for several reasons: the data is shown for only a limited wave vector sample (not averaged for the entire bulk Brillouin zone) and charging effects that remain (not removed in the binding energy corrections to the data [18], in Fermi level placement calibrations) will tend to increase the apparent band gap. Furthermore photoemission and inverse photoemission are final state [38], not initial state spectroscopies, and very surface sensitive.

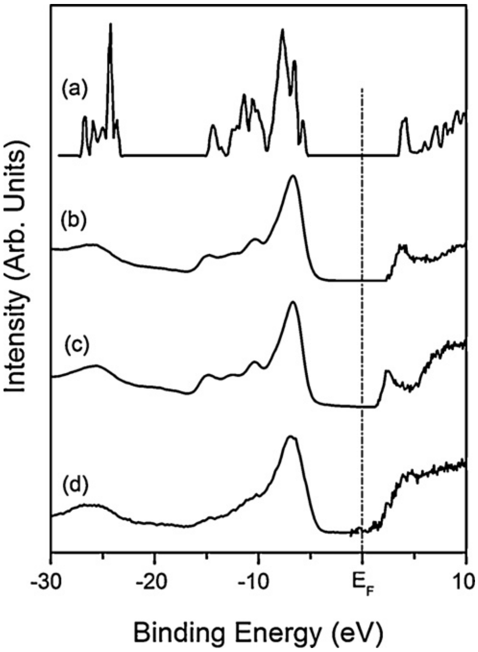

Fig. 1. A comparison of the combined experimental photoemission (left) and inverse photoemission (right) data, in $E - E_F$, with theoretical expectations. The theoretical density of the bulk band states of crystalline $Li_2B_4O_7$ (a) obtained by the LDA PW1PW is adapted from Islam et al. [14]. The combined experimental photoemission (left) and inverse photoemission (right) data for $Li_2B_4O_7$(1 0 0), with the in-plane component of the incident light $\underline{\mathbf{E}}$ for photoemission oriented along [0 1 1] (b) and [0 1 0] (c) are shown along with the data for Cu doped $Li_2B_4O_7$(1 0 0) surface (d). For the photoemission, the synchrotron light is incident at 45° with respect to surface normal. The electrons were either collected along the surface normal (photoemission) or incident along the surface normal (inverse photoemission).

In spite of the numerous deficiencies of the combined photoemission and inverse photoemission experiments, as shown previously [18], the $Li_2B_4O_7$(1 0 0) surface exhibits a density of states that qualitatively resembles that expected from the model bulk band structure of $Li_2B_4O_7$ [14–16], as seen in Fig. 1. Surface contributions, nonetheless, cannot be neglected, and there is now much evidence in support of surface states at the surface of $Li_2B_4O_7$(1 1 0) [18,31]. The Fermi level is placed slightly closer to the conduction band edge in the combined experimental photoemission and inverse photoemission spectra, as seen in Fig. 1. This indicates that the $Li_2B_4O_7$(1 0 0) surfaces are n-type [18]. While we have not measured the majority carrier, the Fermi level placement is consistent with the known bulk properties where the majority of defects seen in nominally undoped $Li_2B_4O_7$(1 0 0) and $Li_2B_4O_7$(1 1 0) were oxygen vacancies [39].

4. The effect of Cu doping of $Li_2B_4O_7$

Electron paramagnetic resonance (EPR) and electron-nuclear double resonance (ENDOR) techniques are well suited to identify and characterize paramagnetic point defects in bulk crystals such as $Li_2B_4O_7$ [39]. Information from hyperfine interactions is especially useful in developing specific models for point defects [39]. Gen-